

RELIABLE DETECTION OF ROTOR FAULTS IN IM USING FREQUENCY TRACKING AND ZERO SEQUENCE VOLTAGE

Khalid DAHI, Soumia EL HANI, Ilias OUACHTOUK

Departement of Electrical Engineering, Ecole Normale Supérieure de l'Enseignement Technique,
Mohammed V University in Rabat, Avenue des Nations Unies, Agdal, Rabat, Morocco

khalid.dahi@um5s.net.ma, s.elhani@um5s.net.ma, ilias_ouachtouk@um5.ac.ma

DOI: 10.15598/aeec.v15i2.2044

Abstract. *The AC Alternating Current Induction Motor (IM) is the most commonly used AC motor in industrial applications because of its simplicity, robust construction, and relatively low manufacturing costs. To avoid expensive repairs in IM, early faults detection is needed. In this context, this paper presents a novel approach used to detect rotor asymmetries in induction motors. The Zero Sequence Voltage (ZSV) defined as the potential difference between the null point of the supply voltage system and the neutral of the star connection of IM stator winding is measured and employed for tracking the amplitude of the most sensitive harmonics in the spectrum of ZSV. This detection leads to make a criterion to take a decision about the state of the machine without a Prior knowledge. Simulation and experimental results obtained from real tests are presented to validate the study.*

Keywords

Frequency tracking, induction motors, rotor fault diagnosis, Zero Sequence Voltage.

1. Introduction

Induction Motors (IM) are used in many industrial processes and are frequently integrated in commercially available equipment. Robustness, cost advantage, high power capabilities, and performance are the major concerns of IM applications. Although IM are reliable, they are subjected to some failures. Therefore, monitoring and diagnosing of IM faults received considerable attention in recent years and it is motivated by objectives for reliability and serviceability in electrical drives [1].

Studies in the area of diagnosis and monitoring of electrical drives have shown that stator and rotor faults are assumed equal [3]. However, the vast majority of articles deal mainly with rotor fault (69 %) first and then with stator faults (30 %) and finally bearing faults [2].

Knowing that the topic is important, this paper deals with rotor fault detection in IMs. This fault that physically result from the short/open circuits or the increase of the rotor resistance. Among the rotor fault accrued in this type of machines we can cite the Broken Rotor Bars (BRBs) in case of machines with squirrel cage.

There are various methods that have been developed to detect BRBs in IMs such as vibration analysis, temperature analysis, acoustic measurement, neuronal and artificial intelligence based methods. However, the most used techniques are based on the monitoring of the stator current spectrum (known as Motor Current Signature Analysis (MCSA) [4], [5] and [6]). Based on that, MCSA is simple and effective in appropriate operating conditions.

Despite the advantages that this method provides, this technique has some significant practical limitations. MCSA is influenced by the operating conditions especially in machine working under very low load. The detection of BRBs is difficult if the IM is supplied by a power converter or if the IM operates in a system under time-varying conditions. An other limitation of MCSA is expressed with recent machines where the IM are frequently installed with inverters which provide some advantages but make the stator current inaccessible to diagnosis [3].

To overcome these limitations, this work proposes the use of Zero Sequence Voltage (ZSV), known also by the Line neutral voltage which is a potential difference between the null point of the supply voltage system and the neutral of the star connection of IM stator winding [8], [10] and [11]. Compared to MCSA, in case

of motor with BRBs, if the slip is very close to zero the frequency that characterizes the fault will not be observable. which is not the case using the ZSV that gives better detection capabilities at no-load condition [9]. It will be shown in this paper that the ZSV contains much more information for IM diagnosis compared to other methods.

In this paper, a new algorithm is proposed aiming at the reliable fault detection of BRBs in IMs. The proposed method is based on the tracking of the amplitude of the most sensitive harmonics in the ZSV spectrum and then apply the proposed criteria to make decision about the IM state. The analysis is performed with the application of the FFT-based method. Experimentation and simulation using Finite Element Model (FEM) [12] and [13] are performed on different motor conditions (Load, number of BRBs, ...).

The structure of this paper is as follows. In Sec. 2, some information are given about the detection of rotor fault in IM using the ZSV. In Sec. 3, the proposed method is theoretically explained. In Sec. 4, we present a validation of the proposed method in both simulation and experimental results. Finally, in Sec. 5, we present some future works and the conclusions of this study.

2. Detection of Rotor Asymmetries Using the ZSV

In [11], the Zero sequence voltage is used to detect short circuit faults in IM by applying an experimental approach without a theoretical analysis. This work goes beyond, since develops a model to detect rotor fault in IM taking into account the ZSV. In Eq. (1), An analytical solution for the ZSV can be obtained for the case when the machine is excited with a balanced supply star connected machine.

$$V_0 = \frac{1}{3}(V_{an} + V_{bn} + V_{cn}). \tag{1}$$

The measurement scheme of ZSV is given in Fig. 1. The ZSV is taking into account by the following mathematical relationship:

$$V_0 = R_a I_{sa} + L_a \frac{dI_{sa}}{dt} + \frac{L_a}{d\theta} \Omega I_{sa} - V_n, \tag{2}$$

where: R_a represents the stator-phase resistance, L_a his inductance, I_{sa} the current passing through it, θ Rotation speed, the angular position of the rotor and V_n supply simple voltage generated by network supply. The presence of a fault rotor reveals additional components in the spectrum of ZSV at frequencies given by

the relation:

$$f_{hdef} = [3h - (3h \pm 1)s] f_s, \tag{3}$$

where s is slip, f_s is supply frequency and h is harmonic order.

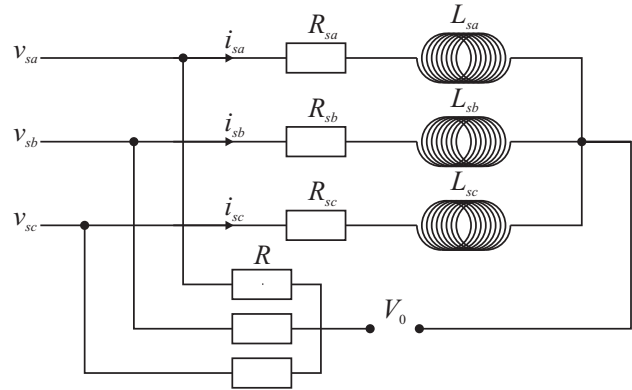


Fig. 1: Zero sequence voltage measurement.

These components computed as derivative of the sum of the three-phase linkage fluxes, appear in case of rotor asymmetry. Experiments are presented in Sec. 4, to correlate the amplitude of the ZSV components to the machine load. The amplitude of these components increases with slip and load conditions.

3. Suggested Methodology - ZSV and FT Combination

In this section, a fault detection criterion based on the combination between the ZSV and the tracking of the important frequencies that characterize the rotor fault in IM is presented. We show that the fault detection criterion can be easily used for this type of fault.

3.1. Problem Formulation

Many methods in the literature are based on the stator current analysis, torque analysis, power analysis, etc [7]. It was shown in [15] using a Finite Element Model, that the Zero Sequence Component (ZSC) can be used to detect and identify rotor fault in induction machine. Also, the amplitudes in ZSC are greater than those of the MCSA as shown in [9].

Most of diagnosis methods used up to now which deals with detection of rotor fault do not provide a direct fault detection criterion. These methods requires the knowledge of the healthy state to make a decision about the rotor.

For that, the proposed harmonic tracking approach is developed using the ZSV as electrical indicator to

detect BRBs without the knowledge of a primary state of the motor. This approach is based on standard deviation calculations taken on two frequency ranges, the first standard deviation will be calculated on the first frequency range, this range identifies where the frequency $(3 - 4s)f_s$. The second standard deviation represent the picture of measurement noise present between frequencies located at $(3 - 4s)f_s$ and $(3 - 6s)f_s$ that is going to be mentioned in this paper as f_{tar1} and f_{tar2} respectively. Finally, using this approach, we are able to generate a decision about the rotor fault which is presented in the end of the proposed method section. It is important to note that The method is valid both for line connected as well as for inverter-fed machines.

Compared to recent works in area of induction machine fault diagnosis, the proposed method is effective and simple to implement because it uses the FFT-based method. Also, the slip of the motor is calculated in each test which is not the case in most recent works [6], [8] and [14].

3.2. Tracking Harmonics Module

As already mentioned, the proposed method is based on the analysis of the frequency $(3 - 4s)f_s$ which is function of the motor slip s . This is why it is necessary to calculate the slip of the IM. The easiest way to do it is the using of a speed sensor in case of experiment test. In this paper we focus on some harmonics to estimate the slip.

In [10], it is demonstrated that the equation given the principal RSH found on the spectrum of the line neutral voltage is given by:

$$f_{RSH} = f_s \left[\lambda \frac{N_r}{p} (1 - s) \pm 1 \right]. \quad (4)$$

The slip can be expressed as:

$$s = 1 - \frac{p}{\lambda N_r} \left[\frac{f_{RSH}}{f_s} \pm 1 \right]. \quad (5)$$

The frequency component $f_s \left[\lambda \frac{N_r}{p} (1 - s) + 1 \right]$ has a much more significant amplitude than the frequency component $f_s \left[\lambda \frac{N_r}{p} (1 - s) - 1 \right]$, which will facilitate its detection.

Practically, all IM have a slight asymmetry of construction induced, in the spectrum of ZSV, the appearance of the frequency component whose frequency equal to $(3 - 2s)f_s$. Therefore, the slip can be expressed from:

$$s = \frac{1}{2} \left[3 - \frac{f_{RSH}}{f_s} \right]. \quad (6)$$

A searching interval is defined because the frequency of the component $(3 - 2s)f_s$ changes according to the load motor; their boundaries depend on the max and min values of the slip s_{min} and s_{max} ; these correspond to unloaded machine and full load machine respectively. Consequently, the searching frequency f_{SR} belongs to the following interval:

$$f_{SR} \in [(3 - 2_{s_{max}})f_s \dots (3 - 2_{s_{min}})f_s]. \quad (7)$$

In our case, given that we know the fundamental frequency f_s , and as our machine is operating with a nominal speed of 2880 rpm which gives a minimum frequency f_{RS} equal to 143.6 Hz, therefore the range selected our detection of this jump will be [140, 150] Hz.

The next step is to identify the value of the $(3 - 2s)f_s$ component and its amplitude in the spectrum of the ZSV, the best way to do this is define a frequency range corresponding to the wanted harmonic, this component which has the highest magnitude nearest the 3rd harmonic in the interval defined as:

$$R = [f_{tar} - i\Delta f; f_{tar} + j\Delta f], \quad (8)$$

where: f_{tar} is target harmonic obtained via the estimated slip, Δf is the frequency resolution ($\Delta f = f_s/N$), i and j are integers. Once the slip is determined.

Next, the idea is to compare the two standard deviation around the f_{tar1} and f_{tar2} frequencies.

$$\begin{aligned} \text{RANGE1} &= \left[(3 - 4s)f_s - \frac{\delta}{2}; (3 - 4s)f_s + \frac{\delta}{2} \right], \\ \text{RANGE2} &= \left[(3 - 4s)f_s - \frac{\delta}{2}; (3 - 6s)f_s + \frac{\delta}{2} \right]. \end{aligned} \quad (9)$$

For an adequate understanding of the principle of calculation of these standard deviations, Fig. 2 shows

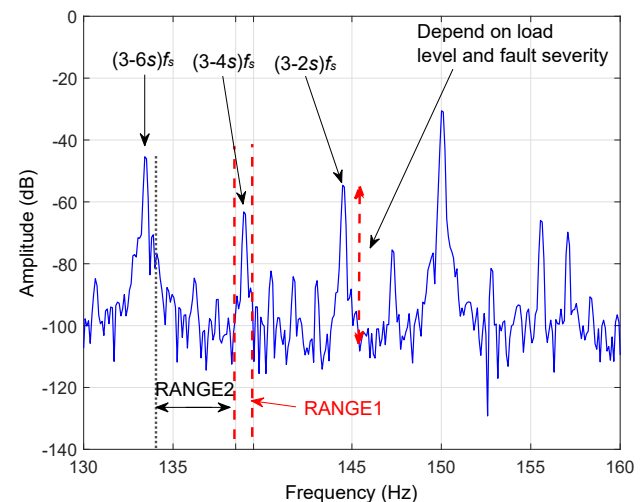


Fig. 2: Explication of the proposed method.

a representation where the standard deviation s_j is calculated on the gray frequency range while the standard deviation s_n is calculated on the black frequency range.

3.3. Design of a Threshold and Decision Making Strategy

In order to make our indicator more robust and to limit false alarms detection, a threshold has been introduced in the criterion that will symbolize with C_{th} . This threshold compares the variance s_j with the variance s_n . Therefore, the authors have defined the following criterion as given in Tab. 1.

Tab. 1: Rotor asymmetry decision module.

Criterion	Rotor State
$C_{RF} \leq C_{th}$	Healthy rotor
$C_{RF} \geq C_{th}$	Defective rotor

Where $C_{RF} = \frac{s_j}{s_n}$, and C_{th} is the sensitivity degree of our fault detection indicator and it is determined in function of the studied IM. Both, the rotor fault index C_{RF} and the corresponding threshold parameter C_{th} are determined from experimental results based on the signal detection theory.

The proposed method can be summarized as follows:

- After acquisition, the ZSV is sampled, and the slip is measured for each case (to be used just for comparison with the estimated slip).
- The slip estimation module is built using Eq. (5) and Eq. (6).
- The estimated slip is used to search the frequency component $(3 - 2s)f_s$ near the 3rd harmonic.
- Once this frequency is estimated, the f_{tar1} and f_{tar2} are estimated too, and the standard deviation in the two ranges is calculated to build the criterion. These values can be compared with pre-defined thresholds to evaluate the machine's condition.

4. Application to IM Rotor Faults Detection

In this section experimental and simulation results are compared. The proposed approach has been implemented in MATLAB-SIMULINK on a DELL Attitude PC, 2 GHz with 4 GB of RAM.

The proposed method will be illustrated using the case of an IM with rotor asymmetry. Nevertheless, the same procedure can be followed to the treatment of any other type of machine fault or working conditions.

4.1. Simulation Results using FE Model of IM

The IM modeling is briefly presented in this section, then the proposed approach is used to detect BRBs faults. IM model for both healthy and faulty motors has been developed based on the Finite Element theory [12], [13], [15] and [16]. The FE field-circuit Model of the IM takes into account the non-linearity of the magnetic materials and is suitable for a deep study of Squirrel Cage Induction Motor (SCIM). It is based on subdivision of the mathematical model into disjoint components of simple geometry called FE, and solving of Maxwell equations by considering the geometry of the structures and properties of the materials.

The basic principle of the FE method applied to electromagnetic calculation is introduced in our previous works [17], by presenting Maxwell's equations first and the dielectric behavior law. We infer from these equations some external parameters such as: the stator currents, Power, torque and the Joule losses.

The magnetic flux is defined as:

$$\varphi = \iint_S \vec{B} \cdot d\vec{S} = \oint_{C(S)} A \cdot dl, \quad (10)$$

where S is any surface, $C(S)$ the closed contour and A a vector potential. The electromagnetic torque is determined by:

$$\Gamma_{em} = R^2 L_z \iint_{2p} H_t B_n dq, \quad (11)$$

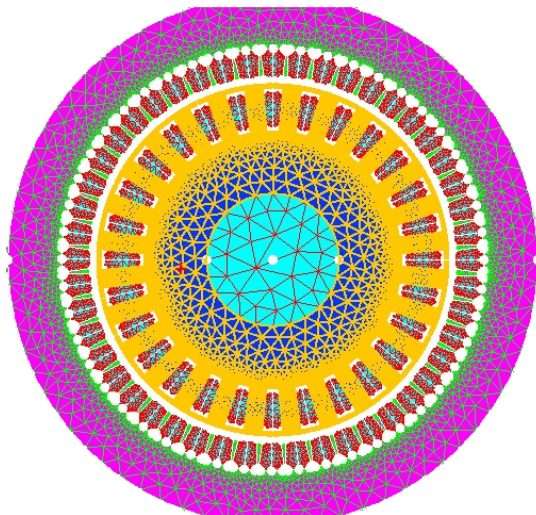
where L_z is the axial length of the machine. The Joule losses density is defined as the scalar product of the electric field and the electric current density. Using the behavior laws used to determine total Joule losses in a volume:

$$pj(t) = \iiint_v \rho \frac{|Jz(t)|^2}{2} dV. \quad (12)$$

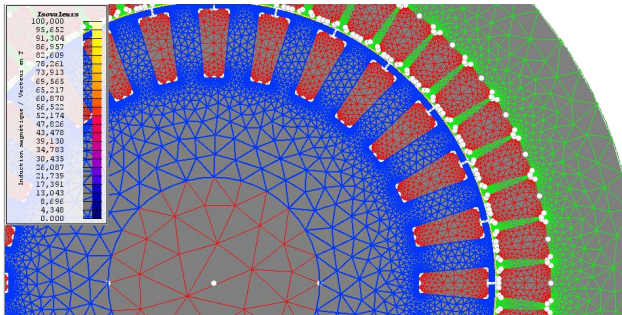
Similarly, the density of magnetic energy is given by the product of the field and of the magnetic induction:

$$\begin{aligned} W_m &= \frac{1}{2} \iiint_v dV \int_0^B h db, \\ &= \frac{1}{2} \iiint_{\text{conductor}} dV \int_0^A j da. \end{aligned} \quad (13)$$

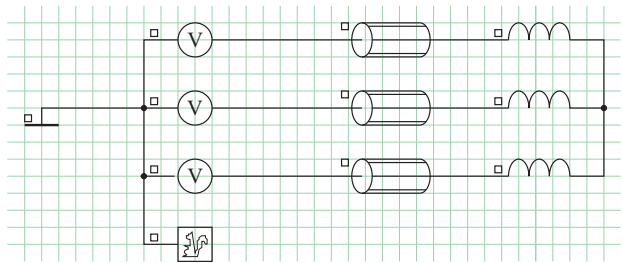
The assignment of elements of the stator and the rotor's electrical circuits to the magnetic circuit is performed interactively using the FLUX2D software. The geometry, the circuit model and the finite element mesh



(a) Geometry.



(b) Mesh zoom.



(c) Electrical circuit model of the IM.

Fig. 3: Finite element model.

in Fig. 3, correspond to a $p = 2$ pole pairs motor of 3 kW, 400 V and $f = 50$ Hz supplied, which is used in the experimental study.

In reality inter bar currents exist in adjacent bars which lead to increase the joule losses. Consequently, in order to model this situation in FE Model, the value of the BB resistance should be selected such that it covers this condition. Furthermore, distribution of the flux lines around the broken bars differs from healthy bars. Since this is not the subject of this work, for more information on modeling using FE, Authors in [14] deals with this subject in details.

In Fig. 4 the rotor currents obtained by the FEM are presented, the results are more accurate, but require more computing time, up to 8 hours in our model.

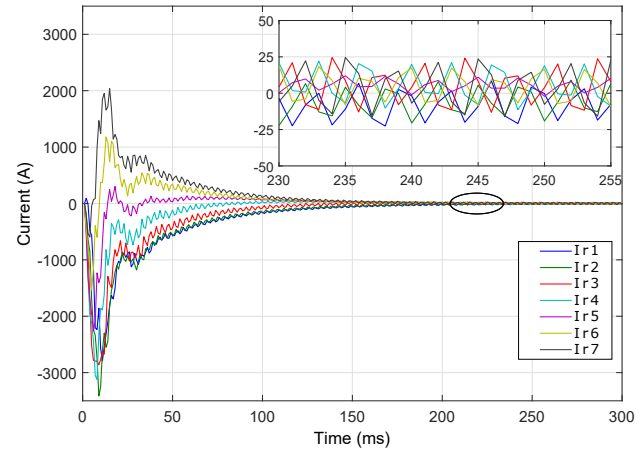


Fig. 4: The rotor currents on an area of 90 degree mechanical (one quarter of the machine).

Figure 5 shows the simulated spectral content of the ZSV – obtained from the FE model – of a healthy and faulty IM operating under rated load at 2889 rpm. In case of faulty IM, the amplitudes of the ZSV odd harmonics increase. Consequently, as seen in Fig. 5 the more appropriate harmonics to be analyzed to diagnose rotor faults is the third harmonic as mentioned in [9].

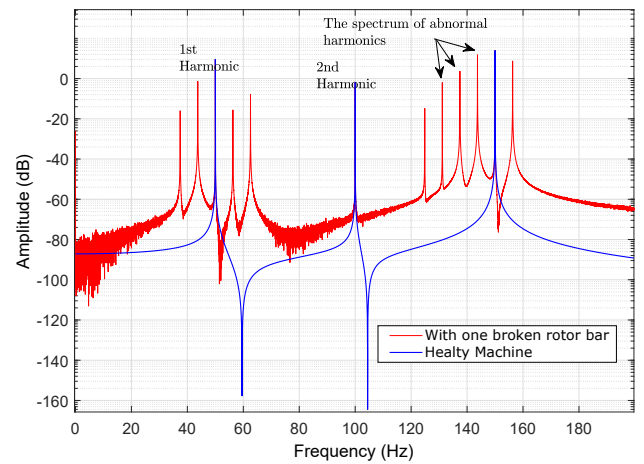


Fig. 5: Simulation: Spectral content of a healthy and faulty machine, operating under 75 % of load.

Table 2 gives the results for BRBs using the proposed technique. The broken bars are adjacent. The criterion has been evaluated for different fault degrees. We can notice that the fault criterion varies in proportion to the number of broken rotor bars and the load conditions. It is worthy to notice that the proposed approach leads to information about faults presence.

We will not present all tests (great execution time), but we focus on tests that will enable us the validation

Tab. 2: Fault detection result of the proposed method.

Supply	Rotor Condition	f_{tar1}	f_{tar1}	Meas. Slip (%)	Est. Slip (%)	s_j	s_n	C_{RF}	Decision
Simulation Results									
	S-H0	145.23	139.19	×	4.77	0.019	0.008	2.44	Healthy
	S-H100	144.9	139.23	×	5.09	0.175	0.058	3.02	Healthy
	S-1bb50	No Max detected							
	S-1bb75	145.41	140.82	×	4.59	0.414	0.036	11.51	Defective
Experimental Results									
Network	S-H0	No Max detected							
	S-H50	145.23	139.19	4.79	4.77	0.384	0.108	3.55	Healthy
	S-H100	144.9	139.23	5.14	5.09	0.105	0.073	1.45	Healthy
	S-1bb0	No Max detected							
	S-1bb25	145.41	140.82	4.63	4.59	0.610	0.067	9.11	Defective
	S-1bb50	144.40	138.81	5.71	5.60	0.15	0.007	21.42	Defective
	S-1bb100	142.33	134.66	3.78	7.67	0.29	0.003	79.30	Defective
	S-2bb0	148.56	147.06	1.47	1.44	0.0316	0.005	6.32	Defective
	S-2bb25	144.37	138.74	5.71	5.63	0.088	0.0082	10.74	Defective
	S-2bb50	143.8	138	6.25	6.2	0.302	0.0063	48.01	Defective
Inverter	S-2bb100	142.95	137.31	7.11	7.05	0.36	0.0062	56.3	Defective
	I-H0	No Max detected							
	I-H100	144.9	139.23	5.14	5.09	0.105	0.073	1.45	Healthy
	I-1bb0	147.40	144.80	2.54	2.61	0.015	0.007	4.89	Defective
	I-1bb75	145.34	140.68	4.72	4.66	2.218	0.093	23.86	Defective

of the proposed method especially test which are figured in the second column of table Tab. 2. Other tests can be seen in the next subsection.

4.2. Experimental Results

Figure 6 shows the structure of the laboratory setup. The motor under test is a 3 kW, 50 Hz, 220/380 V, 2-poles. This motor is directly coupled to a DC machine acting as a load. The sampling frequency was 26 kHz. Voltage and current signals are measured by using LEM Hall sensors. These sensors are connected to the data acquisition board, which is connected to a personal computer.

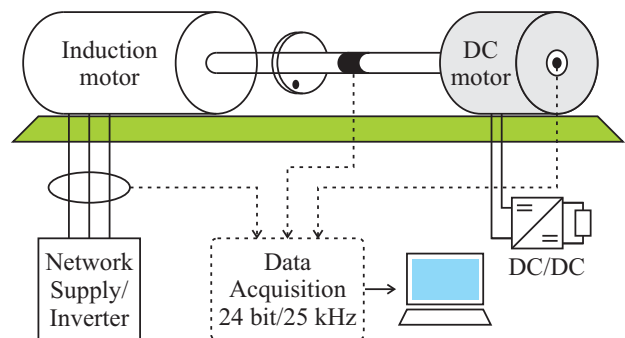
For motor conditions, three types of test motors were used: a healthy motor, a motor with one broken bar and a motor with two broken rotor bars. The motor consists also on inverter which is connected to the load motor in order to connect the load condition of the tested motor.

The measured signals were analyzed by using Fast Fourier Transform (FFT) using a Hanning window to minimize the frequency leakage. For the tested motor, the experiments were performed in the steady state condition to obtain accurate information about the broken rotor bars.

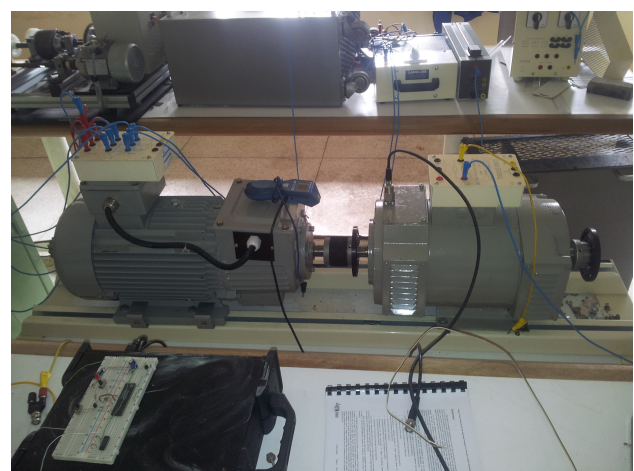
Figure 7 shows the experimental spectrum of the ZSV in healthy and faulty case rated load. It is clear that the 3rd harmonic is appropriate to detect BRBs in IM using ZSV. This supports the simulations results obtained from FE model.

To highlight the sensitivity of the proposed method described in Sec. 3, results shown in Fig. 5 and

Fig. 7 are compared in Tab. 2. The first column in this table corresponds to the machine supply (Line-fed or inverter-Fed), the rotor state is presented in the second column, the third and fourth gives the value of



(a) Block diagram of the studied machine.



(b) The used Induction Machine.

Fig. 6: Experimental setup.

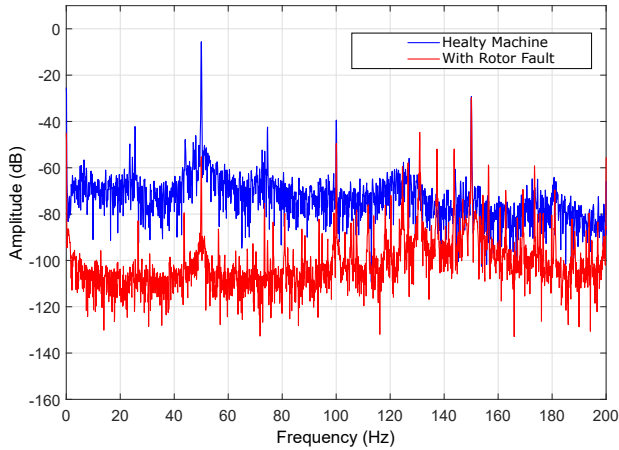


Fig. 7: Experiment: Spectral content of a healthy and faulty machine, operating under 75 % of load.

the frequencies f_{tar1} and f_{tar2} respectively, fifth and sixth column gives the calculated and estimated slip. The values of s_j and s_n calculated on the frequency ranges RANGE1 and RANGE2 are presented in the seventh and eighth column respectively. And then the module decision is presented in the two last columns.

Figure 8 shows an example of the application of the frequency tracking module in the **S-1bb50** case. In the first plot of this figure, Fig. 8(a), the amplitude of target frequencies f_{tar} , f_{tar1} and f_{tar2} can be observed in the ZSV spectrum. In Fig. 8(b), frequency tracking module is shown. It has been built by keeping only the amplitudes of the components of the searched harmonics. For the rest, the same process is done for all tests in Tab. 3.

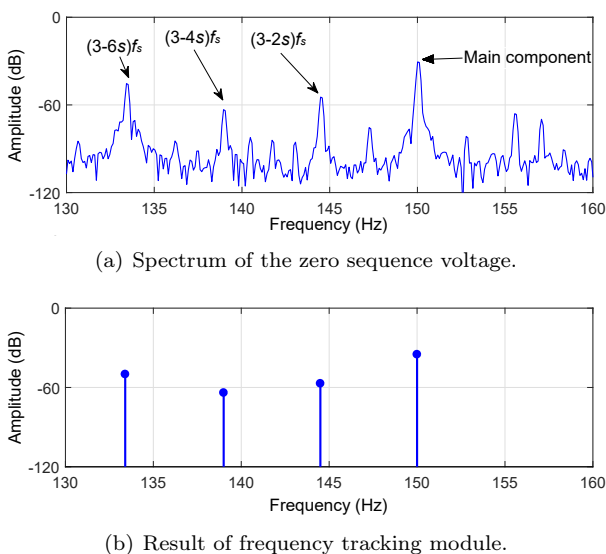


Fig. 8: Experiment: Example of application of the frequency tracking module.

Tab. 3: Experiment details.

Des.	Supply	Details
S-H0	Network	Healthy, unloaded
S-H50		Healthy, under 50% of load
S-H100		Healthy, under 100% of load
S-1bb0		One BRB, unloaded
S-1bb25		One BRB, 25% of load
S-1bb50		One BRB, 50% of load
S-1bb100		One BRB, 100% of load
S-2bb0		Two BRB, unloaded
S-2bb25		Two BRB, 25% of load
S-2bb50		Two BRB, 50% of load
S-2bb100		Two BRB, 100% of load
I-H0		Inverter
I-H100	Healthy, under 100% of load	
I-1bb0	One BRB, unloaded	
I-1bb75	One BRB, 75% of load	

The method described above (Sec. 3.) is applied on the ZSV when the machine is directly star-connected to the three-phase network. According to the column giving C_{RF} , we note that is low for a machine operating with a healthy rotor (**S-H100** and **S-H50**), then we perceive that for some healthy functioning we do not detect the frequency component $(3 - 2s)f_s$. In this case, the rotor is considered in good condition (**S-H0**).

The appearance of a partial rotor fault does not induce a significant increase of s_j relative to s_n , which does not allow to conclude on such a failure. For an important rotor fault (**S-1bb100**), we note that this report is greater 5 times that in tests where the machine is healthy. From these results, it can be concluded that the proposed approach is validated, even if C_{RF} in tests **S-1bb0** and **S-H0** is less pronounced as seen in Tab. 2, but the results are satisfactory.

It is noted that the C_{RF} criterion vary too much despite the variation in the load level. In the defective case a notable variation between fault conditions is seen. From the Tab. 2, C_{RF} does not exceed 5 for a healthy machine and it is greater than 5 for a defective machine.

This conclusion led us to make an IM diagnosis method without reference (this reference usually obtained from a healthy functioning). In other words, if the report s_j/s_n is less than 5 then the machine is healthy, and defective if greater than 5 (as indicated in the last column of Tab. 2). which validate the Tab. 1 where $C_{th} = 5$ for the studied motor.

Results from Tab. 2 show a similar behavior when comparing the simulated results obtained based on FE model proposed in this work with experimental results obtained from real tests. After analyzing these results, the proposed criterion provides sufficiently good sensitivity allowing the detection of rotor asymmetries in IMs.

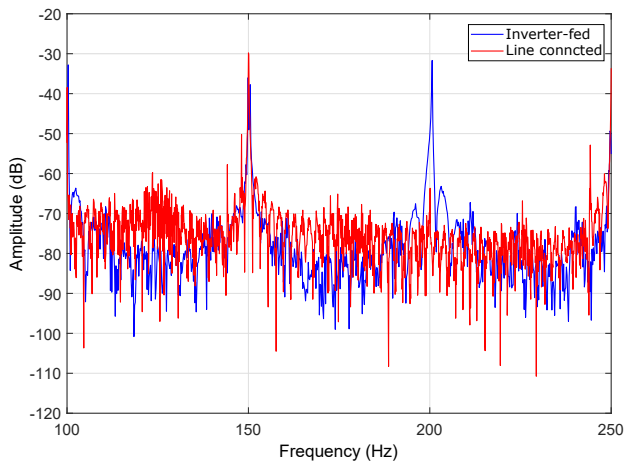


Fig. 9: ZSV in Healthy case with Inverter-fed and line connected machine, operating under 25 % of load.

4.3. Case Study: Induction Machine Supplied by Inverter Fed

The theoretical development of the proposed method, and its comparison with previous approaches, is illustrated with a case study, a 3 kW star-connected induction motor supplied with an inverter, which drives a variable load.

It is well known that in inverted-fed the spectral content of the currents is influenced by the inverter. In [18], it is demonstrated that it is difficult to extract useful information from the study of stator currents of motor in case of inverter-fed because it generates additional harmonics in line current spectrum. On the other hand, the Zero Sequence Voltage based method presented in this paper allows minimizing the additional harmonics on the V_0 spectrum.

After tests, the results are shown in the second part of Tab. 2. If the motor operates at a very low slip (**I-H0**), the diagnosis of this type of fault is especially challenging because the fault harmonics are very close to the mains component and also because the harmonic generated by the inverter as shown in Fig. 9. Compared to other works from the literature, the proposed method gives better results even the machine is supplied with an inverter.

5. Future Research

As mentioned in this paper, the fault index C_{RF} and the threshold criterion C_{th} are determined just from the obtained experimental results. The aim in the next works is to combine the proposed method with the detection probability and the false alarm probability in order to detect rotor faults in IM in order to make a robust condition on C_{th} . Basis of Neyman-Pearson

approach (NPA), see [19] and [20], is that for decision of accepting or rejecting hypothesis in binary case is necessary to consider cost of accepting H_1 and rejection H_0 hypothesis. Using the NPA, the index C_{RF} and the optimal threshold C_{th} in fault decision module will be obtained by:

$$\{C_{RF}, C_{th}\} = \arg\{C_{RF}, C_{th}\} \max \xi_{C_{RF}}, \quad (14)$$

where $\xi_{C_{RF}} = P_{D,C_{RF}} - P_{FA,C_{RF}}$ and:

$$\begin{aligned} P_{D,C_{RF}} &= Pr\{C_{RF} > C_{th}; H_1\}, \\ P_{FA,C_{RF}} &= Pr\{C_{RF} < C_{th}; H_0\}. \end{aligned} \quad (15)$$

Another extension of the proposed method is the detection of multiple faults in IMs is currently under development (eccentricity, bearing fault, ...) and will be presented in a future paper.

6. Conclusion

In this paper, an affective approach to detect rotor fault in IM has been proposed, it is based on the analysis of a new fault indicator that uses both the harmonic tracking and the Zero sequence voltage. The presented indicator allows to have a knowledge about the rotor state, the fault severity and the corresponding slip for the data acquisition. With the proposed method, the decision making is done. It was shown that this approach -in addition that it is easy to implement- provides some advantages over existing methods in the literature:

- Robustness and efficiency under time-varying operating conditions.
- The proposed method has a high sensitivity to detect rotor fault.

The description of the proposed method, its theoretical justification, Simulation and the experimental validation are fully confirmed under a wide variety of supply types and working conditions.

References

- [1] CAPOLINO, G. A., J. A. ANTONINO-DAVIU and M. RIERA-GUASP. Modern Diagnostics Techniques for Electrical Machines, Power Electronics, and Drives. *IEEE Transactions on Industrial Electronics*. 2015, vol. 62, iss. 3, pp. 1738–1745. ISSN 0278-0046. DOI: 10.1109/TIE.2015.2391186.
- [2] NAHA, A., A. K. SAMANTA, A. ROUFRAY and A. K. DEB. A Method for Detecting

- Half-Broken Rotor Bar in Lightly Loaded Induction Motors Using Current. *IEEE Transactions on Instrumentation and Measurement*. 2016, vol. 65, iss. 7, pp. 1614–1625. ISSN 0018-9456. DOI: 10.1109/TIM.2016.2540941.
- [3] FILIPPETTI, F., A. BELLINI and G. A. CAPOLINO. Condition monitoring and diagnosis of rotor faults in induction machines: State of art and future perspectives. In: *IEEE Workshop on Electrical Machines Design Control and Diagnosis (WEMDCD)*. Paris: IEEE, 2013, pp. 196–209. ISBN 978-1-4673-5656-5. DOI: 10.1109/WEMDCD.2013.6525180.
- [4] THOMSON, W. T. and M. FENGER. Current signature analysis to detect induction motor faults. *IEEE Industry Applications Magazine*. 2001, vol. 7, iss. 4, pp. 26–34. ISSN 1077-2618. DOI: 10.1109/2943.930988
- [5] JUNG, J.-H., J.-J. LEE and B.-H. KWON. Online Diagnosis of Induction Motors Using MCSA. *IEEE Transactions on Industrial Electronics*. 2006, vol. 53, iss. 6, pp. 1842–1852. ISSN 1557-9948. DOI: 10.1109/TIE.2006.885131.
- [6] LEE, S. B., D. HYUN, T.-J. KANG, C. YANG, S. SHIN, H. KIM, S. PARK, T.-S. KONG and H.-D. KIM. Identification of False Rotor Fault Indications Produced by Online MCSA for Medium-Voltage Induction Machines. *IEEE Transactions on Industry Applications*. 2016, vol. 52, iss. 1, pp. 729–739. ISSN 0093-9994. DOI: 10.1109/TIA.2015.2464301.
- [7] DAHI, K., S. EL HANI, S. GUEDIRA, I. OUACHTOUK and A. ECHCHAACHOUAI. Diagnosis of rotor asymmetries in Induction motor using ESA. In: *2016 International Conference on Electrical and Information Technologies (ICEIT)*. Tangiers: IEEE, 2016, pp. 1–8. ISBN 978-1-4673-8469-8. DOI: 10.1109/EITech.2016.7519564.
- [8] GYFTAKIS, K. N., J. A. ANTONINO-DAVIU, R. GARCIA-HERNANDEZ, M. D. MCCULLOCH, D. A. HOWEY and A. J. MARQUES CARDOSO. Comparative Experimental Investigation of Broken Bar Fault Detectability in Induction Motors. *IEEE Transactions on Industry Applications*. 2016, vol. 52, iss. 2, pp. 1452–1459. ISSN 0093-9994. DOI: 10.1109/TIA.2015.2505663.
- [9] GARCIA, P., F. BRIZ, M. W. DEGNER and A. B. DIEZ. Diagnostics of induction machines using the zero sequence voltage. In: *IEEE Industry Applications Conference*. Seattle: IEEE, 2004, pp. 735–742. ISBN 0-7803-8486-5. DOI: 10.1109/IAS.2004.1348496.
- [10] OUMAAMAR, M. E. K., A. KHEZZAR, M. BOUCHERMA, H. RAZIK, R. N. ANDRIAMALALA and L. BAGHLI. Neutral Voltage Analysis for Broken Rotor Bars Detection in Induction Motors Using Hilbert Transform Phase. In: *42nd Annual Meeting of the IEEE-Industry-Applications-Society*. New Orleans: IEEE, 2007, pp. 1940–1947. ISBN 978-1-4244-1259-4. DOI: 10.1109/07IAS.2007.295.
- [11] CASH, M. A., T. G. HABETLER and G. B. KLIMAN. Insulation failure prediction in AC machines using line-neutral voltages. *IEEE Transactions on Industry Applications*. 1998, vol. 34, iss. 6, pp. 1234–1239. ISSN 0093-9994. DOI: 10.1109/28.738983
- [12] FERKOVA, Z. Comparison between 2D and 3D Modelling of Induction Machine Using Finite Element Method. *Advances in Electrical and Electronic Engineering*. 2015, vol. 13, no. 2, pp. 120–126. ISSN 1804-3119. DOI: 10.15598/aeee.v13i2.1346.
- [13] WALLACE, A. K. and A. WRIGHT. Novel Simulation of Cage Windings Based on Mesh Circuit Model. *IEEE Transactions on Power Apparatus and Systems*. 1974, vol. PAS-93, iss. 1, pp. 377–382. ISSN 0018-9510. DOI: 10.1109/TPAS.1974.293957.
- [14] BOUGHRARA, K., N. TAKORABET, R. IBTIOUEN, O. TOUHAMI and F. DUBAS. Analytical Analysis of Cage Rotor Induction Motors in Healthy, Defective, and Broken Bars Conditions. *IEEE Transactions on Magnetics*. 2015, vol. 51, iss. 2, pp. 1–17. ISSN 0018-9464. DOI: 10.1109/TMAG.2014.2349480.
- [15] GYFTAKIS, K. N. and J. C. KAPPATOU. The Zero-Sequence Current as a Generalized Diagnostic Mean in Delta-Connected Three-Phase Induction Motors. *IEEE Transactions on Energy Conversion*. 2014, vol. 29, no. 1, pp. 138–148. ISSN 0885-8969. DOI: 10.1109/TEC.2013.2292505.
- [16] SINGH, A., B. GRANT, R. DEFOUR, C. SHARMA and S. BAHADOORSINGH. A review of induction motor fault modeling. *Electric Power Systems Research*. 2016, vol. 133, iss. 1, pp. 191–197. ISSN 0378-7796. DOI: 10.1016/j.epsr.2015.12.017.
- [17] OUACHTOUK, I., S. E. HANI, S. GUEDIRA, L. SADIKI and K. DAHI. Modeling of squirrel cage induction motor a view to detecting broken rotor bars faults. In: *1st International Conference on Electrical and Information Technologies*. Marrakech: IEEE, 2015, pp. 347–352. ISBN 978-1-4799-7479-5. DOI: 10.1109/EITech.2015.7163001.

- [18] ROUX, W. L., R. G. HARLEY and T. G. HABETLER. Detecting faults in rotors of PM drives. *IEEE Industry Applications Magazine*. 2008, vol. 14, iss. 2, pp. 23–31. ISSN 1077-2618. DOI: 10.1109/MIA.2007.915789.
- [19] CHARFI, F., S. LESECQ and F. SELLAMI. Fault diagnosis using SWT and Neyman Pearson detection tests. In: *IEEE International Symposium on Diagnostics for Electric Machines, Power Electronics and Drives*. Cargese: IEEE, 2009, pp. 1–6. ISBN 978-1-4244-3440-4. DOI: 10.1109/DEMPED.2009.5292788.
- [20] MUSTAFA, M. O., D. VARAGNOLO, G. NIKOLAKOPOULOS and T. GUSTAFSSON. Detecting broken rotor bars in induction motors with model-based support vector classifiers. *Control Engineering Practice*. 2016, vol. 52, iss. 1, pp. 15–23. ISSN 0967-0661. DOI: 10.1016/j.conengprac.2016.03.019.

About Authors

Khalid DAHI was born in Errachidia, Morocco, in 1988. He received the M.Sc. degree in electrical engineering in 2012 from the Mohammed V University in Rabat- Morocco. Where he is currently working toward the Ph.D. degree in the department of electrical engineering. Since 2012, His research interests are related to electrical machines and drives, diagnostics of induction motors. His current activities include monitoring and diagnosis of induction machines in wind motor.

Soumia EL HANI has been Professor at the ENSET (Ecole Normale Supérieure de l'Enseignement Technique - Rabat, Morocco) since October 1992. She is a Research Engineer at the Mohammed V University in Rabat Morocco, in charge of the research team electromechanical, control and diagnosis, IEEE member, member of the research laboratory in

electrical engineering at ENSET - Rabat. Author of several publications in the field of electrical engineering, including robust control systems, diagnosis and control systems of wind electric conversion. She has been general co-Chair the two editions of "the International Conference on Electrical and Information Technologies", held in Marrakech, March 2015 and Tangier, May 2016 respectively.

Ilias OUACHTOUK was born in Fom Zguid-Tata, Morocco, in 1991. He received his M.Sc. degree in electrical engineering from the Mohammed V University in Rabat, Morocco, in 2014. Where he is currently working toward the Ph.D. degree, in the department of electrical engineering. Since 2015. His research interests include modeling and diagnosis of electrical drives, in particular, synchronous and asynchronous motors.

Appendix A Induction Motor Parameters

- $P_N = 3 \text{ kW}$,
- $U_{1N} = 220 \text{ V}$,
- $f_s = 50 \text{ Hz}$,
- $p = 2$,
- $N_r = 28$,
- $R_s = 1.5 \Omega$,
- $R_b = 96.9 \cdot 10^{-6} \Omega$,
- $L_b = 0.28 \cdot 10^{-6} \text{ H}$,
- $L_e = 0.036 \cdot 10^{-6} \text{ H}$,
- $j = 4\pi \cdot 10^{-7} \frac{\text{W}_b}{\text{A} \cdot \text{m}}$.